34th Annual International Conference of the IEEE EMBS
San Diego, California USA, 28 August - 1 September, 2012

Real-time Performance of a Hands-free Semi-autonomous Wheelchair System Using a Combination of Stereoscopic and Spherical Vision

Jordan S. Nguyen, Tuan Nghia Nguyen, Yvonne Tran, Steven W. Su,
Ashley Craig, and Hung T. Nguyen, *Senior Member, IEEE*

***Abstract*—This paper is concerned with the operational performance of a semi-autonomous wheelchair system named TIM (Thought-controlled Intelligent Machine), which uses cameras in a system configuration modeled on the vision system of a horse. This new camera configuration utilizes stereoscopic vision for 3-Dimensional (3D) depth perception and mapping ahead of the wheelchair, combined with a spherical camera system for 360-degrees of monocular vision. The unique combination allows for static components of an unknown environment to be mapped and any surrounding dynamic obstacles to be detected, during real-time autonomous navigation, minimizing blind-spots and preventing accidental collisions with people or obstacles. Combining this vision system with a shared control strategy provides intelligent assistive guidance during wheelchair navigation, and can accompany any hands-free wheelchair control technology for people with severe physical disability. Testing of this system in crowded dynamic environments has displayed the feasibility and real-time performance of this system when assisting hands-free control technologies, in this case being a proof-of-concept brain-computer interface (BCI).**

I. INTRODUCTION

PHYSICAL mobility impairment, in many cases, can result in fewer socializing and leisure opportunities, decreased pursuits of goals, loss of physical independence, and heightened risk of depression in sufferers. Mobility aids, such as electric-powered wheelchairs, can provide significant improvements to the quality of life for many people living with physical disability. However, safe control of conventional powered wheelchairs require from the user significant levels of skill, attention, and judgment [1]. Accidents are always a potential risk when using wheelchairs and can cause injuries if they occur.

Recent decades have seen great advancements in the development of autonomous and semi-autonomous powered wheelchairs, placing them in the category of 'smart wheelchairs'. Some popular examples of these advancements, featuring shared-control strategies developed for various wheelchair platforms, include *SENA* [2], *Rolland* [3], *Hephaestus* [4], and *Navchair* [5]. However, these wheelchairs do not facilitate operation in unknown dynamic environments, either requiring prior knowledge about the environment or not being able to combine with data about the local environment. Furthermore, these systems require further development for reliable real-time operation.

Robotics techniques play a large role in intelligent system design, and as such are incorporated into smart wheelchair development. Many modern artificial sensors used in intelligent robotic applications are biologically inspired and modeled on real sensors in living systems such as humans, animals, and insects [6]. In this paper, we present the real-time operational performance from the testing of a semi-autonomous wheelchair system that utilizes a novel combination of stereoscopic and spherical vision cameras in a manner that has been inspired by the equine visual system.

As previously documented [7], the wheelchair's vision system being modeled on equine vision allows for the stereoscopic vision to map static objects ahead of the wheelchair in real-time and use obstacle avoidance strategies for both static and dynamic objects. The spherical vision, in addition, provides dynamic obstacle detection all around the wheelchair, preventing collisions with moving objects which have not already been mapped.

This wheelchair is aimed at assisting people with severe disabilities, and is able to interface with any hands-free control technology, such as BCIs. Through the development of multivariable control strategies, the wheelchair provides automated guidance assistance and obstacle avoidance, allowing safe navigation to assist hands-free control. Testing was conducted in a crowded environment, using a BCI for control, to assess the real-time performance of the designed vision configuration and automated guidance system. This paper focuses on the automated guidance assistance strategies and real-time operation of the wheelchair in combination with the selected hands-free control technology.

In Section II of this paper, aspects of the biologically inspired vision system and assistive navigation strategies are provided. Section III presents results and discussions of the real-time performance of the overall designed system which incorporates multivariable control and automated guidance assistance. Section IV concludes this paper.

II. DESIGN AND DEVELOPMENT

A. Stereoscopic and Spherical Vision Combination

As previously reported [7], the biological inspiration for this wheelchair is equine vision system. The novel combination of stereoscopic cameras and spherical vision cameras mimics the binocular and monocular fields of view inherent in the equine visual system, whilst also minimizing the blind spots (Fig. 1).

This work was supported in part by Australian Research Council under Discovery Grant DP0666942 and LIEF Grant LE0668541.

Jordan S. Nguyen is with the Faculty of Engineering and Information Technology, University of Technology, Sydney, Broadway, NSW 2007, Australia (phone: +612-9514-4441; fax: +61 2 9514 2868; e-mail: Jordan.Nguyen@uts.edu.au).

Ashley Craig is with the Rehabilitation Studies Unit, Faculty of Medicine at University of Sydney, Australia.

Tuan Nghia Nguyen, Yvonne Tran, Steven W. Su, and Hung T. Nguyen are with the Faculty of Engineering and Information Technology, University of Technology, Sydney, Broadway, NSW 2007, Australia.

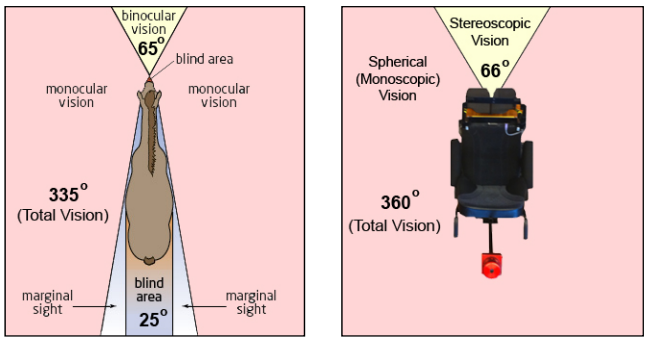

Fig. 1: Visual System of a Horse (left); Wheelchair Vision Design (right)

The stereoscopic cameras at the front of the wheelchair provide approximately 66º of vision similar to the binocular vision of a horse, and the spherical vision cameras above the back of the wheelchair provide complete 360º monoscopic vision, similar to the monocular vision of the horse without the posterior blind spots. This allows 3D mapping of the local environment ahead of the wheelchair and detection of obstacles posing as potential collision dangers (dynamic in particular) all around the wheelchair.

The purpose of stereo vision is to perform range measurements based on the left and right images obtained from stereoscopic cameras. In order to produce a disparity image, the Sum of Absolute Differences (SAD) correlation algorithm in Eq.1 is used to compare a neighborhood of pixels in one stereo image to a number of neighborhoods in the other stereo image [8],

$$SAD = \min_{d=d_{\min}}^{d_{\max}} \sum_{i=-M}^{+M} \sum_{j=-M}^{+M} \left| I_R(x+i, y+j) - I_L(x+i+d, y+j) \right|, \quad (1)$$

where a window of size $(2M+1)\times(2M+1)$ (correlation mask) is centered at the coordinates of the matching pixels (i, j), (x, y) in one stereo image, I_L and I_R are the intensity functions of the left and right images, and d_{min}, d_{max} are the minimum and maximum disparities. The disparity d_{min} of zero pixels often corresponds to an infinitely far away object and the disparity d_{max} denotes the closest position of an object. Once a disparity image is produced from the processed left and right camera images, a 3D point map can be created which maps the depth-determined pixels from the disparity image into a 3D plane[8].

The Ladybug2 camera configuration consists of five cameras around and one on top to allow for complete 360°, and more than 80% of the full sphere, in spherical vision around and above the system [9]. This is useful in this project for detecting obstacles located within the safety zones of the wheelchair which may obstruct movement or rotation in the corresponding directions [7].

B. TIM-VPH Obstacle Avoidance Algorithm

The obstacle avoidance algorithm investigated for this application was the Vector Polar Histogram (VPH) method [10], which was a combination, adaptation, and improvement of both the Potential Field Method (PFM) [11] and the Enhanced Vector Field Histogram (VFH+) [12]. PFM and VFH+ were primarily developed for mobile robotic obstacle avoidance applications using sonar and ultrasonic sensors, whereas VPH was adapted for use with laser rangefinders. Since the TIM smart wheelchair utilizes camera systems for environmental perception, the VPH algorithm, with the integration of some VFH+ concepts, has been adapted and improved again for this application, which will be referred to here as TIM-VPH.

The TIM-VPH method here takes on the general structure of the VPH algorithm, replaces some concepts with those of VFH+, and makes improving adaptations to suit the equine vision-inspired camera configuration used by the TIM smart wheelchair. A producer-consumer control loop was deployed whereby the hands-free control commands from the user, such as via BCI controls, are acquired through its own timed 'producer' loop, and the command data is then sent to the TIM wheelchair's data processing and control 'consumer' loop. The producer loop typically runs at a slightly faster rate than the consumer loop, thus resulting in the consumer loop utilizing only the most recently transmitted data. After image acquisition and processing from the two camera systems has completed in each cycle, the instantaneous local environment obstacle map is updated accordingly. Following this map update, the main steps of the TIM-VPH algorithm, all still included in the consumer loop, are:

1. Convert the 'active area' (being the local updating range of the environment map) to a grid form, similar to VFH+ except with binary values representing free or occupied cells, as opposed to certainty values.

$$\begin{aligned} m_{x,z} &= 0 \quad if \quad cell\ is\ empty \\ m_{x,z} &= 1 \quad if \quad cell\ is\ occupied\ by\ object \end{aligned} \quad (2)$$

2. Safety to a single point (Fig. 2). This is another included VFH+ expansion of objects and reduction of wheelchair representation concept, adapted here to a non-circular model representation, since the TIM wheelchair model is more adequately represented by a rectangle. Without this step the rectangular model representation would otherwise present further problems, in dimensional accountability, for the algorithms providing automated obstacle-avoiding navigational maneuvers.

3. Goal direction creation whenever a command is given to the wheelchair. A target cell can placed at the nearest object location in the goal direction or further past the objects in the goal direction, depending on what the user commands. As with all other active obstacle cells, the vector

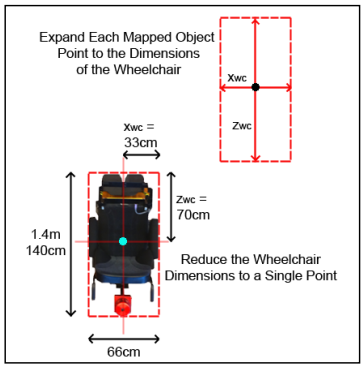

Fig. 2: TIM representation reduction and correlating object expansion

direction and magnitude from the wheelchair centre point (WCCP) can be found as follows:

Vector direction of active cell from wheelchair centre point:

$$\beta_{x,z} = arctan\left(\frac{z_{ac} - z_{wccp}}{x_{ac} - x_{wccp}}\right) \quad (3)$$

Vector distance of active cell from wheelchair centre point:

$$d_{x,z} = \sqrt{\left(x_{ac} - x_{wccp}\right)^2 + \left(z_{ac} - z_{wcpp}\right)^2} \quad (4)$$

where: (x_{wccp}, z_{wccp}) = coordinates of the WCCP
(x_{ac}, z_{ac}) = coordinates of active cell

4. Creation of a vector polar histogram. Sector segmentation is done to convert the active area matrix into a polar histogram displaying closest object distance as opposed to obstacle density for each sector, with any sectors that do not contain objects within sight being allocated the maximum vision range distance d_{v_max} away from the wheelchair, indicating large amounts of free space in that direction. For each sector corresponding to each direction angle α (here being 0 to 180 degrees), the polar obstacle magnitude is the distance to the nearest object for that sector $d_{x,z}(\alpha)$, which represents the maximum distance $D(\alpha)$ in that direction that the wheelchair can reach. This is defined as:

$$D(\alpha) = \min\left(d_{x,z}(\alpha)\right) \qquad \alpha = 0,1,2,\ldots,180 \quad (5)$$

5. Reduction of the polar histogram by threshold function into a binary histogram providing candidate directions for possible navigation. As in VPH this takes into account the wheelchair's real-time velocity, acceleration and deceleration parameters, allowing the necessary time and space to stop the wheelchair to be obtained:

$$t = \frac{V(t)}{a} \quad , \quad S(t) = V(t)a - \frac{1}{2}at^2 = \frac{V^2(t)}{2a} \quad (6)$$

For each direction angle α, the function can be rewritten as:

$$V(\alpha,t) = \frac{\boldsymbol{V_t}.\boldsymbol{d_1}}{D(\alpha,t)} = \begin{cases} V_t.cos^2(\theta(t) - \alpha) & ; \ |\theta(t) - \alpha| \le 90 \\ 0 & ; \ |\theta(t) - \alpha| > 90 \end{cases}$$

$$S(\alpha,t) = \frac{V^2(\alpha,t)}{2a} = \begin{cases} \frac{V_t^2.cos^2(\theta(t) - \alpha)}{2a} & ; \ |\theta(t) - \alpha| \le 90 \\ 0 & ; \ |\theta(t) - \alpha| > 90 \end{cases}$$

Then, taking into consideration an additional general safety distance between wheelchair and obstacles (D_s), we define a time-varying threshold function for each angle as:

$$D_T(\alpha,t) = S(\alpha,t) + D_s \quad (7)$$
$$= \begin{cases} \frac{V_t^2.cos^2(\theta(t) - \alpha)}{2a} + D_s & ; \ |\theta(t) - \alpha| \le 90 \\ D_s & ; \ |\theta(t) - \alpha| > 90 \end{cases}$$

where:
V_t is the real-time speed of the wheelchair,
$\theta(t)$ is the steering direction of the wheelchair,
a is the deceleration of the wheelchair.

By comparing the polar histogram and the threshold function, a binary histogram can be produced, which is created using the following:

$$H(\alpha,t) = 1 \qquad if\ D(\alpha,t) \ge D_T(\alpha,t)$$
$$H(\alpha,t) = 0 \qquad if\ D(\alpha,t) < D_T(\alpha,t) \quad (8)$$

6. Selection of a steering direction from candidate directions, being those where $H(\alpha,t) = 1$, producing a set of candidate angles U. This is adapted and improved from the VPH method. An appropriate cost function C is used to select a direction Ω from the candidate angles, and is represented as a function of each candidate angle α belonging to candidate angles set U. Unlike smaller mobile robotics, in larger applications such as this TIM smart wheelchair, passing as close as possible to obstacles is not necessary. So for this reason, as well as the fact that candidate directions exhibiting a larger amount of free space are more desirable, a cost inversely proportional to the amount of free space up to the maximum vision range distance d_{v_max} is added to the candidate direction cost function.

$$C(\alpha) = K_1|\alpha - \varphi| + K_2|\alpha - \theta| + K_3\left(\frac{D}{d_{v\_max}}\right) \quad , \quad \alpha \in U \quad (9)$$

where:
K_1, K_2, K_3 are constants,
φ is the target direction of the wheelchair.

The first term represents the cost associated with deviating from the target direction. The second term represents the cost associated with deviating away from the current heading direction. The third term represents the cost associated with directions that have obstacles up ahead, which will reduce with more free space in any given direction. The constants are undetermined parameters that will facilitate the level of importance placed on each of the associated term.

The best direction is the one that has the least associated cost value, representing the most appropriate balance between the cost terms. So the final selection of steering direction Ω is found as follows:

$$C(\Omega) = \min\ C(\alpha), \ \alpha \in U \quad (10)$$

7. Speed control is based on the distance to objects in the selected steering direction Ω, found from Eq. 10, and will range up to the maximum allowed speed V_{max}:

$$V = \left(1 + \frac{d_{v\_max} - d(\Omega)}{d_{v\_max} - D_s}\right)V_{max} \quad (11)$$

III. RESULTS

Experiments were conducted at the University of Technology, Sydney (UTS) in the main area of the tower building during peak lunch hours when there were many people walking around. The aim of these experiments were to test the performance of TIM's assistive guidance capabilities when navigating through a crowded and highly dynamic environment from one area to another, past pre-defined checkpoints, whilst being controlled via hands-free control technology. For these experiments, trialed by an able-bodied person, a proof-of-concept BCI was used for control through EEG signal classifications. Although, with respect to many BCIs in research, this was a reasonably simple interface, shared-control with the assistive guidance of the TIM smart wheelchair provided adequate control for safely directing the wheelchair through each of the checkpoints.

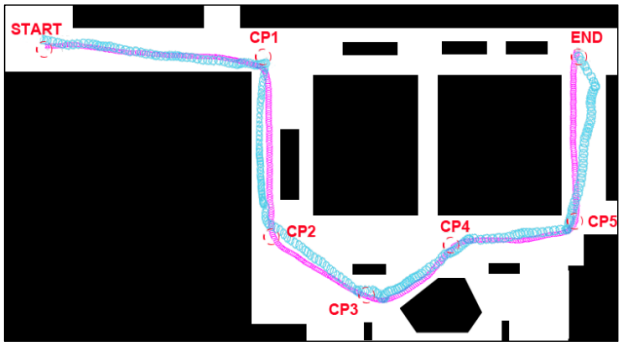

Fig. 3: Location Map: Joystick (Pink) vs BCI+TIM (Blue) Paths Executed

From the Start point (CP0) to the End destination (CP6), there were five other checkpoints (CP1-CP5) that had to be passed along the way as displayed in Fig. 3. This was first run using a joystick to control the power wheelchair (Pink path in Fig. 3) with a consistent speed of V_{max} for comparison purposes. For this comparative trial the total distance traveled was about 110m, completed in a total time of 182seconds. This meant an average speed of 0.6m/s.

Eight trials were then conducted using the BCI for control and TIM's navigational guidance (BCI+TIM), with the first of these runs being displayed as the blue path in Fig. 3. Completion times varied, mostly due to the crowd density (Fig. 4) as TIM slowed down and consumed more time when avoiding people in crowded areas, with times between check points shown in Fig. 5. Overall, however, the use of BCI in shared-control with TIM's navigational guidance only took an average of slightly more than double the time taken to complete the course using the conventional joystick (Fig. 6).


Fig. 4: Photos of "BCI+TIM Trial 1" Navigating Through UTS Crowds

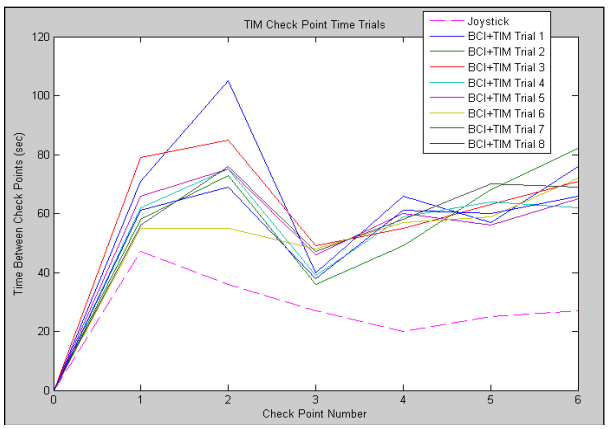

Fig. 5: TIM Check Point Time Trial Intervals

	Trials: J = Joystick, Others = BCI+TIM Trial #								
	J	1	2	3	4	5	6	7	8
Total Time (sec)	182	415	366	402	361	368	346	376	355
Avg Speed (m/s)	0.6	0.27	0.30	0.27	.30	0.30	0.32	0.29	0.31

Fig. 6: Total Time and Average Speed for Trial Runs

IV. CONCLUSION

This system has shown that the unique combination of both stereoscopic cameras and spherical vision cameras can be used to allow a semi-autonomous wheelchair to assist the user with effective guidance assistance when navigating in unknown, crowded, and dynamic indoor environments. The equine-inspired vision combination allows for both static objects and environmental attributes to be mapped as well as dynamic obstacles such as people walking past to be detected. Automated navigation and obstacle avoidance strategies allow the safe maneuvering of the wheelchair through these environments.

These results have shown that the combination of stereoscopic and spherical vision cameras, along with personalized obstacle avoidance algorithms, can assist hands-free control systems, including difficult systems such as BCIs. They have also displayed the ability, in the designs and developments of the TIM smart wheelchair, to handle navigation in crowded environments through 3D mapping from the stereoscopic cameras and 360º obstacle zone classification from the spherical vision cameras. This will lead onto full experimental trials with tetraplegic patients from the Royal Rehabilitation Centre in Sydney (RRCS).

REFERENCES

[1] A. Mihailidis, P. Elinas, J. Boger, and J. Hoey, "An Intelligent Powered Wheelchair to Enable Mobility of Cognitively Impaired Older Adults: An Anticollision System", *IEEE Transactions on Neural Systems and Rehabilitation Engineering*, vol. 15, pp. 136-143, 2007.

[2] C. Galindo, J. Gonzalez, and J. A. F-Madrigal, "Control Architecture for Human-Robot Integration: Application to a Robotic Wheelchair", *IEEE Trans. on Systems, Man, and Cybernetics*, pp. 1053-1067, 2006.

[3] A. Lankenau, and T. Rofer, "A versatile and safe mobility assistant", *IEEE Robotics and Automation Magazine*, vol. 8, pp. 29-37, 2001.

[4] R. C. Simpson, D. Poirot, F. Baxter, "The Hephaestus Smart Wheelchair System", *IEEE Trans. on Neural Systems and Rehab. Eng.*, vol. 10, no. 2, 2002.

[5] S. P. Levine, D. A. Bell, A. J. Lincoln, R . C. Simpson, Y. Koren, J. Borenstein, "The NavChair Assistive Wheelchair Navigation System", *IEEE Transactions on Rehabilitation Engineering*, vol. 7, no. 4, 1999.

[6] P. Dario, M. C. Carrozza, L. Beccai, C. Laschi, B. Mazzolai, A. Menciassi, and S. Micera, "Design, fabrication and applications of biomimetic sensors in biorobotics", *Proceedings of the IEEE International Conference on Information Acquisition*, pp.263-266, 2005.

[7] J. S. Nguyen, Y. Tran, S. W. Su, and H. T. Nguyen, "Semi-autonomous Wheelchair Developed Using a Unique Camera System Configuration Biologically Inspired by Equine Vision", *33rd Annual International Conference of the IEEE Engineering for Medicine and Biology Society*, pp. 5762 – 65, 2010.

[8] J. S. Nguyen, T. H. Nguyen, and H. T. Nguyen, "Semi-autonomous Wheelchair System Using Stereoscopic Cameras", *31st Annual International Conference of the IEEE Engineering for Medicine and Biology Society*, pp. 5068-5071, 2009.

[9] J. S. Nguyen, S. W. Su, and H. T. Nguyen, "Spherical Vision Cameras in a Semi-autonomous Wheelchair System", *32nd Annual International Conference of the IEEE Engineering for Medicine and Biology Society*, pp. 4064 – 4067, 2010.

[10] D. An, and H. Wang, "VPH: A New Laser Radar Based Obstacle Avoidance Method for Intelligent Mobile Robots", *Proceedings of the 5th World Congress on Intelligent Control and Automation*, pp. 4681-4685, 2004.

[11] J. Borenstein and Y. Koren, "Real-time Obstacle Avoidance for Fast Mobile Robots", *IEEE Transactions on Systems, Man, and Cybernetics*, vol. 19, no. 5, pp. 1179-1187, 1989.

[12] J. Gong, Y. Duan, Y. Man, and G. Xiong, "VPH+: An Enhanced Vector Polar Histogram Method for Mobile Robot Obstacle Avoidance", *Proceedings of the 2007 IEEE Conference on Mechatronics and Automation*, pp 2784-2788, 2007.